



EDGEWOOD

CHEMICAL BIOLOGICAL CENTER

U.S. ARMY RESEARCH, DEVELOPMENT AND ENGINEERING COMMAND

ECBC-TR-638

VAPOR-PHASE INFRARED ABSORPTIVITY COEFFICIENT OF *BIS*-(2-CHLOROETHYL) SULFIDE

Barry R. Williams
Melissa S. Hulet



SCIENCE APPLICATIONS
INTERNATIONAL CORPORATION
Abingdon, MD 21009

Alan C. Samuels
Ronald W. Miles
Frederic J. Berg
Leslie McMahon
H. Dupont Durst

RESEARCH AND TECHNOLOGY DIRECTORATE

July 2008

Approved for public release;
distribution is unlimited.



20081001431

ABERDEEN PROVING GROUND, MD 21010-5424

Disclaimer

The findings of this report are not to be construed as an official Department of the Army position unless so designated by other authorizing documents.

REPORT DOCUMENTATION PAGE				Form Approved OMB No. 0704-0188	
Public reporting burden for this collection of information is estimated to average 1 hour per response, including the time for reviewing instructions, searching existing data sources, gathering and maintaining the data needed, and completing and reviewing this collection of information. Send comments regarding this burden estimate or any other aspect of this collection of information, including suggestions for reducing this burden to Department of Defense, Washington Headquarters Services, Directorate for Information Operations and Reports (0704-0188), 1215 Jefferson Davis Highway, Suite 1204, Arlington, VA 22202-4302. Respondents should be aware that notwithstanding any other provision of law, no person shall be subject to any penalty for failing to comply with a collection of information if it does not display a currently valid OMB control number. PLEASE DO NOT RETURN YOUR FORM TO THE ABOVE ADDRESS.					
1. REPORT DATE (DD-MM-YYYY) XX-07-2008		2. REPORT TYPE Final		3. DATES COVERED (From - To) Mar 2008 - Apr 2008	
4. TITLE AND SUBTITLE Vapor-Phase Infrared Absorptivity Coefficient of <i>Bis</i> -(2-Chloroethyl) Sulfide				5a. CONTRACT NUMBER	
				5b. GRANT NUMBER	
				5c. PROGRAM ELEMENT NUMBER	
6. AUTHOR(S) Williams, Barry R.; Hulet, Melissa S. (SAIC); Samuels, Alan C.; Miles, Ronald W.; Berg, Frederic J.; McMahon, Leslie; and Durst, H. Dupont (ECBC)				5d. PROJECT NUMBER None	
				5e. TASK NUMBER	
				5f. WORK UNIT NUMBER	
7. PERFORMING ORGANIZATION NAME(S) AND ADDRESS(ES) Science Applications International Corporation, 3465A Box Hill Corporate Drive, Abingdon, MD 21009 DIR, ECBC, ATTN: AMSRD-ECB-RT-DP, APG, MD 21010-5424				8. PERFORMING ORGANIZATION REPORT NUMBER ECBC-TR-638	
9. SPONSORING / MONITORING AGENCY NAME(S) AND ADDRESS(ES)				10. SPONSOR/MONITOR'S ACRONYM(S)	
				11. SPONSOR/MONITOR'S REPORT NUMBER(S)	
12. DISTRIBUTION / AVAILABILITY STATEMENT Approved for public release; distribution is unlimited.					
13. SUPPLEMENTARY NOTES					
14. ABSTRACT-LIMIT 200 WORDS We measured the vapor-phase absorptivity coefficient of the vesicant chemical warfare agent, <i>bis</i> -(2-chloroethyl) sulfide (HD), in the mid-infrared (4000-550 cm ⁻¹) at a spectral resolution of 0.125 cm ⁻¹ . The HD used in the feedstock was subjected to a rigorous analysis by gas chromatography (GC) and NMR to verify its purity, and the vapor used to produce the composite spectrum was periodically sampled by GC. In this report, we describe the experimental method employed to acquire the individual spectra that were used to produce the composite spectrum, summarize the statistical uncertainties in the data, and provide a comparison to similar data from another laboratory.					
15. SUBJECT TERMS Infrared FTIR Absorptivity coefficient Quantitative Vapor-phase HD Mustard Vapor pressure Saturator cell					
16. SECURITY CLASSIFICATION OF:			17. LIMITATION OF ABSTRACT	18. NUMBER OF PAGES	19a. NAME OF RESPONSIBLE PERSON
a. REPORT	b. ABSTRACT	c. THIS PAGE			Sandra J. Johnson
U	U	U	UL	29	19b. TELEPHONE NUMBER (include area code) (410) 436-2914

Blank

EXECUTIVE SUMMARY

We measured the vapor-phase absorptivity coefficient of *bis*-(2-chloroethyl) sulfide (HD) in the mid-infrared. We used agent filled saturator cells suspended in a temperature controlled liquid bath to generate continuous streams of HD diluted in nitrogen. The cells were sent to a variable path White cell and measured using a high resolution research grade Fourier transform infrared spectrometer. The purity of the feedstock was verified by gas chromatography (GC) and NMR. The concentration of HD in the vapor was determined with a gravimetric method, and the vapor generated was sampled periodically by GC. Ten spectra at different concentration-pathlength products were processed line by line through least squares analysis using MatLab® to produce the absorptivity coefficient of the compound and the statistical uncertainty in the data. Uncertainties in the data, expanded to a confidence interval of 2σ ($P=0.95$), are Type-A (4%) and Type-B (4.2%) of the absorptivity coefficient. In this report, we report a comparison of our data to that obtained by another laboratory using a different vapor generation method.

Blank

PREFACE

The work described in this report was performed under the direction of the Detection Capability Officer (DCO), Defense Threat Reduction Agency (DTRA) Joint Science and Technology Office (JSTO). This work was started in March 2008 and completed in April 2008.

The use of either trade or manufacturers' names in this report does not constitute an official endorsement of any commercial products. This report may not be cited for purposes of advertisement.

This report has been approved for public release. Registered users should request additional copies from the Defense Technical Information Center; unregistered users should direct such requests to the National Technical Information Service.

Acknowledgments

This work was performed under the direction of the DCO, DTRA JSTO. Kenneth Sumpter and David McGarvey (U.S. Army Edgewood Chemical Biological Center) and William Creasy (Science Applications International Corporation), members of the Chemical Methodologies Team, assisted with the analysis of the feedstock material for the acquisition of data used in preparing this report.

Blank

CONTENTS

1.	INTRODUCTION	11
2.	EXPERIMENTAL SECTION	11
2.1	Instrumental Details	11
2.2	Feedstock	12
3.	RESULTS AND DISCUSSION	13
4.	INTERLABORATORY COMPARISON	19
5.	CONCLUSIONS.....	27
	LITERATURE CITED	29

FIGURES

1.	Structure of <i>bis</i> -(2-chloroethyl) Sulfide.....	11
2.	Beer's Law Plot of 1212.5 cm ⁻¹ Line in the Vapor-Phase Spectrum of <i>bis</i> -(2-chloroethyl) Sulfide	13
3.	Beer's Law Plot of 720.6 cm ⁻¹ Line in the Vapor-Phase Spectrum of <i>bis</i> -(2-chloroethyl) Sulfide	14
4.	Absorptivity Coefficient of <i>bis</i> -(2-chloroethyl) Sulfide	15
5.	Uncertainty in the Absorptivity Coefficient of <i>bis</i> -(2-chloroethyl) Sulfide	15
6.	Absorption Coefficient and Type-A Uncertainty, Fractional, 2σ, for HD.....	16
7.	Absorption Coefficient and Type-A Uncertainty, 2σ for HD.....	17
8.	Absorptivity Coefficients of Vapor-Phase HD from ECBC and PNNL.....	20
9.	Absorptivity Coefficient Spectra of HD Vapor from ECBC and PNNL.....	20
10.	Absorptivity Coefficient Spectra from ECBC and PNNL.....	21
11.	Vapor-Phase Absorptivity Coefficients of HD from PNNL and ECBC, and the Liquid Absorptivity Coefficient.....	23
12.	Vapor-Phase Absorptivity Coefficients of HD from PNNL and ECBC, and the Liquid Absorptivity Coefficient.....	23
13.	Vapor-Phase Absorptivity Coefficients of HD from PNNL after Spectral Subtraction and ECBC, and the Liquid Absorptivity Coefficient	24
14.	Vapor-Phase Absorptivity Coefficients of HD from PNNL after Spectral Subtraction and ECBC, and the Liquid Absorptivity Coefficient	24
15.	Band at 1037 cm ⁻¹ in Vapor-Phase Spectra of HD from PNNL and ECBC and Liquid-Phase Spectrum from PNNL.....	26

TABLES

1.	Absorptivity Coefficient of <i>bis</i> -(2-chloroethyl) Sulfide for Selected Bands	16
2.	Type-A Statistical Uncertainty for HD Vapor-Phase Absorptivity Coefficient	18
3.	Uncertainties in Absorptivity Coefficient of HD from ECBC Data where $\alpha \geq 0.0000716 \text{ (}\mu\text{mol/mol)}^{-1}\text{m}^{-1}$	18
4.	Ratios of CH to C-Cl in Vapor-Phase Spectrum from ECBC and Spectrally Subtracted Spectrum from PNNL	25
5.	Comparison of Integrated Vapor-Phase Absorptivity Coefficient Spectrum of HD from PNNL and ECBC	26

Blank

VAPOR-PHASE INFRARED ABSORPTIVITY COEFFICIENT OF *BIS*-(2-CHLOROETHYL) SULFIDE

1. INTRODUCTION

We have obtained the high resolution vapor-phase absorptivity coefficients of the vesicant, *bis*-(2-chloroethyl) sulfide (HD), in the spectral range of 4000-550 cm^{-1} in units of $(\mu\text{mol/mol})^{-1}\text{m}^{-1}$, and additionally made an initial computation of the uncertainties of the data. Previous efforts at the U.S. Army Edgewood Chemical Biological Center (ECBC) to obtain the absorptivity coefficients of HD date back to the 1960s and were performed at lower resolution on a grating spectrometer.¹ Given the extensive use of vapor-phase infrared spectra for the standoff detection of chemical warfare agents (CWAs), the need for current data is apparent.

For HD, the Chemical Abstracts Service Registry Number is 505-20-2, the molecular formula is $\text{C}_4\text{H}_8\text{Cl}_2\text{S}$, and the molecular weight is 159.08. Synonyms for the compound include 2,2'-dichloroethyl sulfide, 1,1'-thio-*bis*-(2-chloroethane), sulfur mustard, Levinstein mustard, and S-lost. The structure of HD is shown in Figure 1.

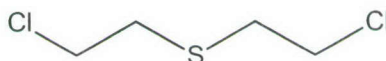


Figure 1. Structure of *bis*-(2-chloroethyl) Sulfide (HD)

Bis-(2-chloroethyl) sulfide is a delayed action vesicant CWA that was first employed in combat during WWI. It has a freezing point of 14.45 °C and a vapor pressure of 0.069 Torr (9.2 Pa) at 20 °C.²

2. EXPERIMENTAL SECTION

2.1 Instrumental Details.

The system used to generate the continuous vapor stream was an adaptation of the saturator cell method developed at ECBC for measuring the volatility of CWA related compounds.³

The method, modified to generate continuous streams of chemical compounds for obtaining quantitative vapor-phase infrared spectra, has been used to measure the absorptivity coefficients of benzene⁴ and a variety of CWA related compounds.⁵ References 4 and 5 describe the experimental setup, as well as the data collection and post-processing in more detail. The saturator passes a stream of nitrogen carrier gas, obtained from the boil-off of a bulk liquid nitrogen tank, across a conical alumina wicking mechanism in a glass holder filled with the analyte. A saturated vapor-liquid equilibrium of the analyte on the downstream side of the

saturator cell results with the concentration of the analyte determined by the temperature of the liquid phase. By suspending the saturator cell in a constant temperature bath, the concentration of the analyte can be predicted by its vapor pressure at the temperature of the bath. The apparatus used in the Quantitative Fourier transform infrared (FTIR) Laboratory uses a Brooks Model 5850S mass flow controller to maintain a constant flow to the saturator cell, along with a second mass flow controller to add diluent to the stream, providing an additional means of adjusting the concentration of the compound delivered to the White cell of the FTIR. Linearity of the S series mass flow controllers is adjusted using a second order polynomial, resulting in accuracies of approximately 1% or a better rate at flows $\geq 25\%$ of full scale.

Spectra were obtained with a Bruker Model IFS/66V FTIR spectrometer. The instrument was equipped with both deuterated triglycine sulfide and mercury-cadmium-telluride (HgCdTe) detectors and is capable of obtaining spectra with a maximum spectral resolution of 0.1125 cm^{-1} (unapodized). The interferograms were recorded from $15798\text{--}0\text{ cm}^{-1}$ with a resolution of 0.125 cm^{-1} . Absorbance (log base-10) spectra were processed with boxcar apodization and 2X zero filled to obtain a data spacing of 0.0625 cm^{-1} . The instrument was equipped with a variable path White cell. The experimental data used path lengths of 4.057 and 8.024 m. The temperature of the White cell was maintained at $23 \pm 0.1\text{ }^{\circ}\text{C}$ through the use of a thermostatically controlled chamber enclosing the spectrometer and cell. Data were acquired at a speed of 60 KHz (HeNe laser zero crossing frequency) using the HgCdTe detector. Single beam spectra of the CWA were ratioed against spectra of clean, dry nitrogen. To minimize the effects of nonlinearity in the detector, the interferograms were processed using the proprietary Opus® nonlinearity correction function. All interferograms were archived enabling further post-processing of data.

Temperature and pressure data were recorded using the National Institute of Standards and Technology (NIST) traceable digital manometers and thermometers, and all data were archived. Concentration-pathlength (CL) products were computed in units of $\mu\text{mol/mol(m)}$ (ppm-m). A differential pressure manometer had previously been used to measure the dynamic pressure in the White cell with gas flowing into the cell, and the ambient pressure was plotted versus the differential pressure. The resulting equation was used to correct the readings from the ambient pressure manometer to the pressure in the White cell. The CL data were corrected to 296 K and $1.0132 \times 10^5\text{ Pa}$ (760 Torr) using the ideal gas law.

2.2 Feedstock.

The material used to generate the vapor streams for the experiments was obtained from the Chemical Sciences Team at ECBC, with a reported purity of 99% (NMR and GC-Mass Spectrometry).

We verified the purity of the feedstock using GC with a flame ionization detector (FID) at 98.9%. The primary impurity was 1,4-dithiane at 1.1% by weight. We additionally checked the purity of the effluent vapor from the White cell by thermal desorption GC-FID. In the effluent, 1,4-Dithiane was observed.

3. RESULTS AND DISCUSSION

Four trials were run to obtain spectra at 10-CL products. A trial is defined as filling and weighing the saturator cell, suspending it in the bath, applying a stream of nitrogen for a measured time, acquiring several spectra, stopping the nitrogen and removing it from the bath, and reweighing the saturator cell after drying the exterior surfaces and re-equilibrating to room temperature. The first trial was conducted with the saturator cell suspended in a water bath maintained at 23.3 °C, with the remaining trials at 24.0 °C.

Trace water vapor was removed from the spectra by spectral subtraction. In the spectra, 1,4-dithiane was also observed. The concentration of the compound in the vapor was computed using the absorptivity coefficient of 1,4-dithiane obtained in our laboratory, and the features of the impurity were removed by spectral subtraction. Baseline corrections were performed with several spectra using a two point linear subtraction. The correction in no case exceeded 0.001 A [$A = -\log_{10}(T)$].

The composite spectrum (absorptivity coefficient) was computed using spectra with CL products ranging between 207-849 $\mu\text{mol/mol(m)}$ (corrected to 296 K and 101325 Pa). As an initial check of the quality of the data, Beer's Law plots of two spectral lines, 1212.5 and 720.6 cm^{-1} , were calculated using MatLab®, showing that, at least for these two spectral lines, the data appeared to be well fitted, with no points lying outside the 95% confidence limits for either a repeated set or a repeated single X, or the 95% confidence limits for a Grubbs Test for Outliers⁶ (Figures 2 and 3).

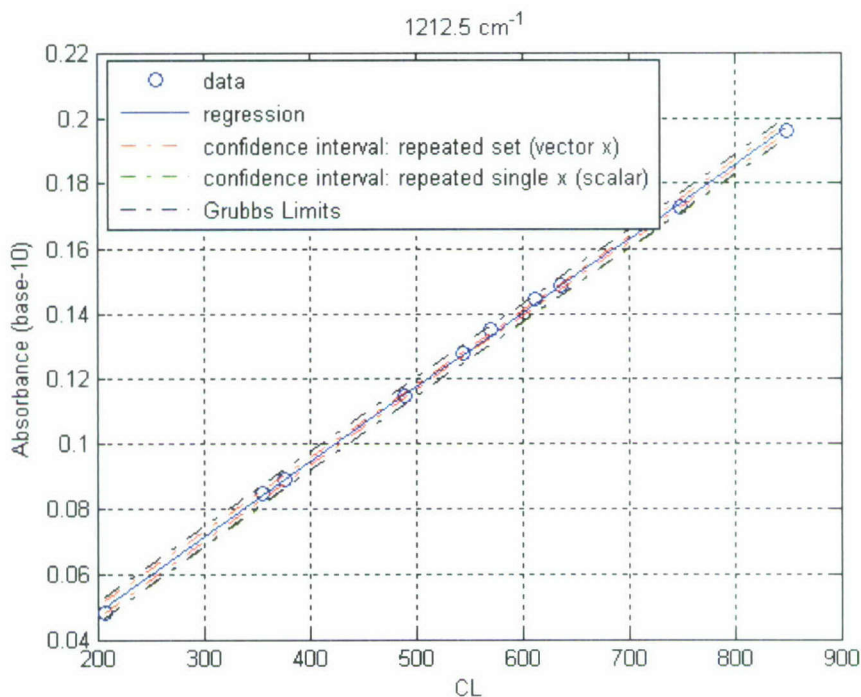


Figure 2. Beer's Law Plot of 1212.5 cm^{-1} Line in the Vapor-Phase Spectrum of bis-(2-chloroethyl) Sulfide

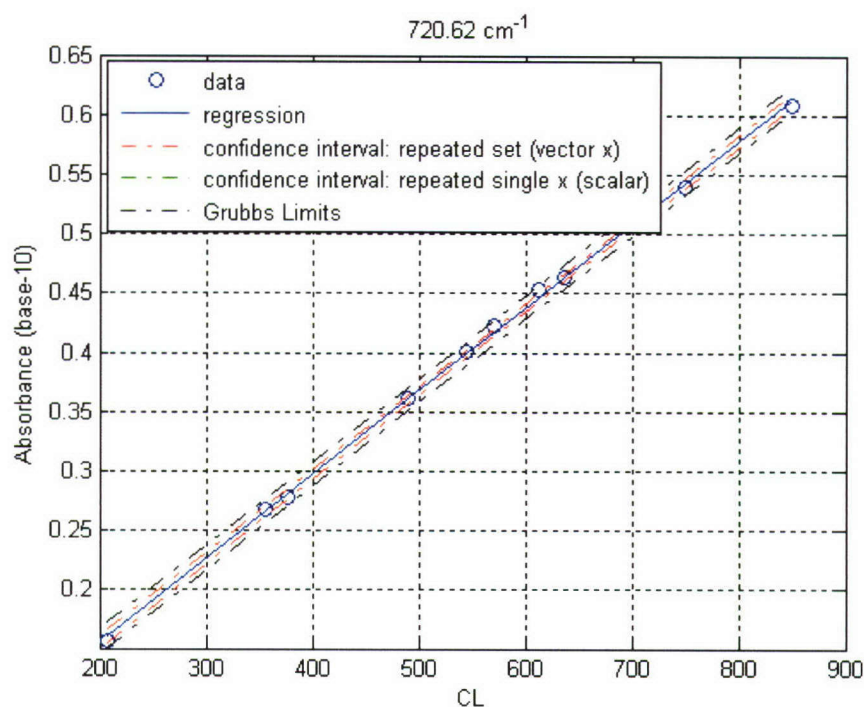


Figure 3. Beer's Law Plot of 720.6 cm⁻¹ Line in the Vapor-Phase Spectrum of *bis*-(2-chloroethyl) Sulfide

The absorptivity coefficient (α) and uncertainty (Type-A, 2σ) were computed line by line within the spectral range of 4000-550 cm⁻¹ using a MatLab program written in-house. Values of ($A = -\log T$) > 1.5 are normally assigned a weight of zero. Because A did not exceed 0.615, all values of A were weighted at one. Figure 4 is the plotted absorptivity coefficient (α), and Figure 5 is the Type-A uncertainty for the computed spectral range. The figures are plotted with α in (μmol/mol)⁻¹m⁻¹. To obtain α in (mg/m²)⁻¹, multiply the values in the mantissa of Figure 4 by 0.1518. This factor is derived from eq 1 using the molecular weight of HD (159.08)

$$\frac{m^2}{mg} \left(\frac{24.15}{mw} \right) = \frac{mol}{\mu mol(m)} \quad (1)$$

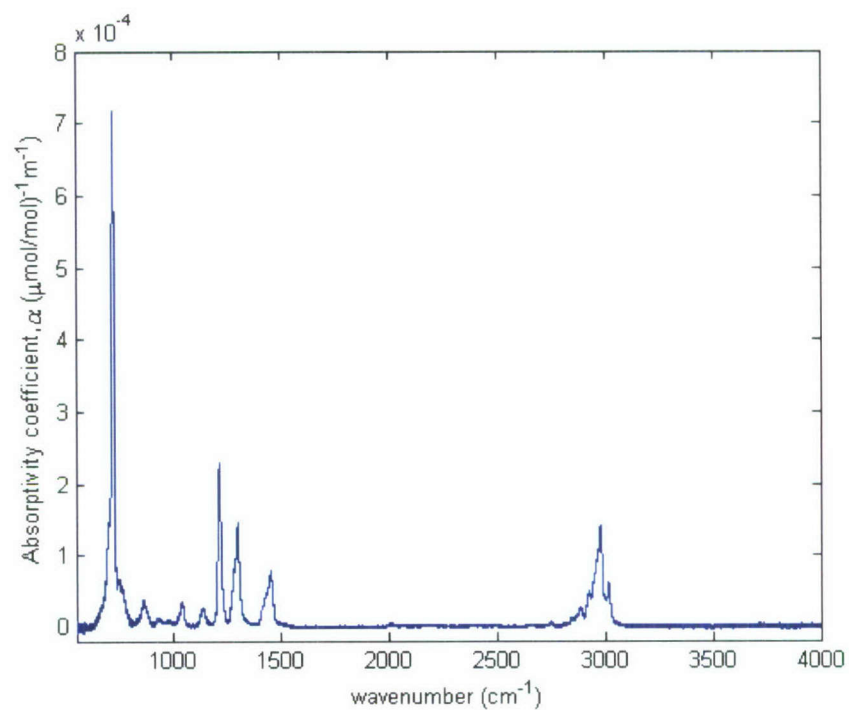


Figure 4. Absorptivity Coefficient of *bis*-(2-chloroethyl) Sulfide

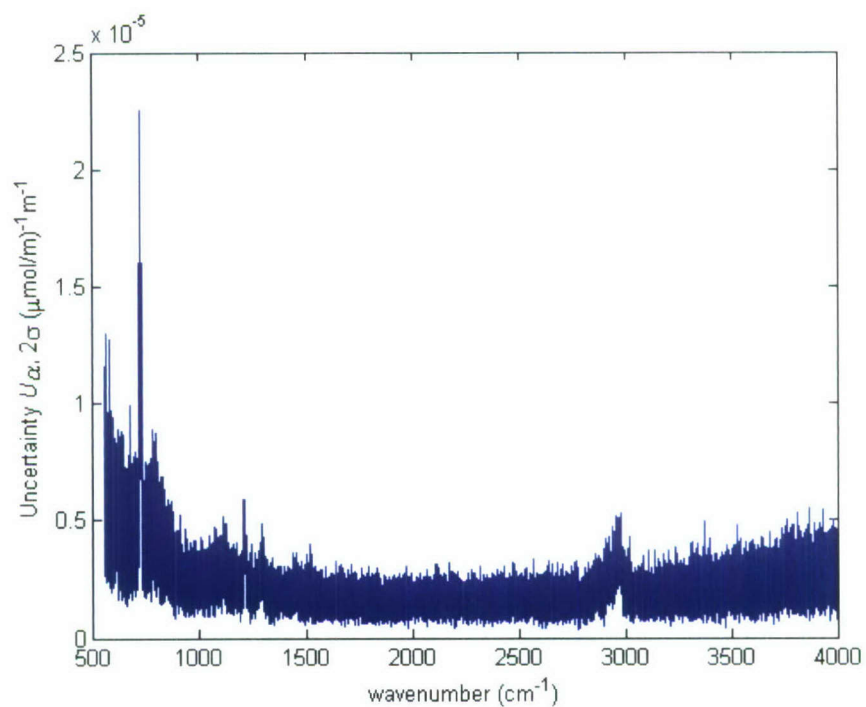


Figure 5. Uncertainty in the Absorptivity Coefficient of *bis*-(2-chloroethyl) Sulfide (Type-A, 2σ)

Table 1 provides the absorptivity coefficients in $(\mu\text{mol/mol})^{-1}\text{m}^{-1}$ and $(\text{mg/m}^2)^{-1}$ for selected bands in units of wavenumber and micrometers (μm).

Table 1. Absorptivity Coefficient of *bis*-(2-chloroethyl) Sulfide for Selected Bands

Wavenumber, cm^{-1} (Wavelength, μm)	Absorptivity coefficient, $(\mu\text{mol/mol})^{-1}\text{m}^{-1}$ [(mg/m^2) $^{-1}$]
1299.25 (7.70)	1.141E-04 (2.19E-05)
1212.41 (8.25)	2.291E-04 (3.477E-05)
1037.16 (9.64)	3.460E-05 (5.25E-06)
720.59 (13.88)	7.117E-04 (1.08E-04)

In general, expanded type-A uncertainties were 2-3% of the absorptivity coefficient, as seen in Figures 6 and 7. Figure 6 is a plot of absorptivity coefficients (abscissa) and fractional uncertainty (Type-A, U_A , 2σ) (mantissa). Figure 7 is a plot of the absorptivity coefficient and uncertainty and also includes a best fit of the data points obtained by least squares, which is an approximation of $U_A \approx ax+b$. For the fitted line in Figure 7, the coefficients are $a = 1.72 \times 10^{-2}$ and $b = 2.03 \times 10^{-6}$ (Table 2).

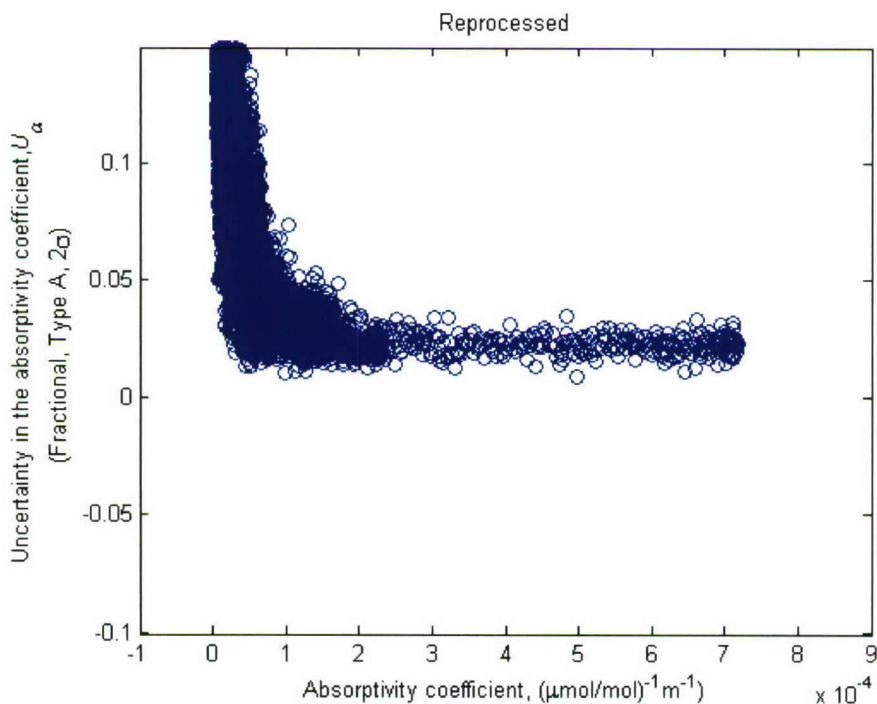


Figure 6. Absorption Coefficient (Abscissa) and Type-A Uncertainty, Fractional, 2σ , for HD

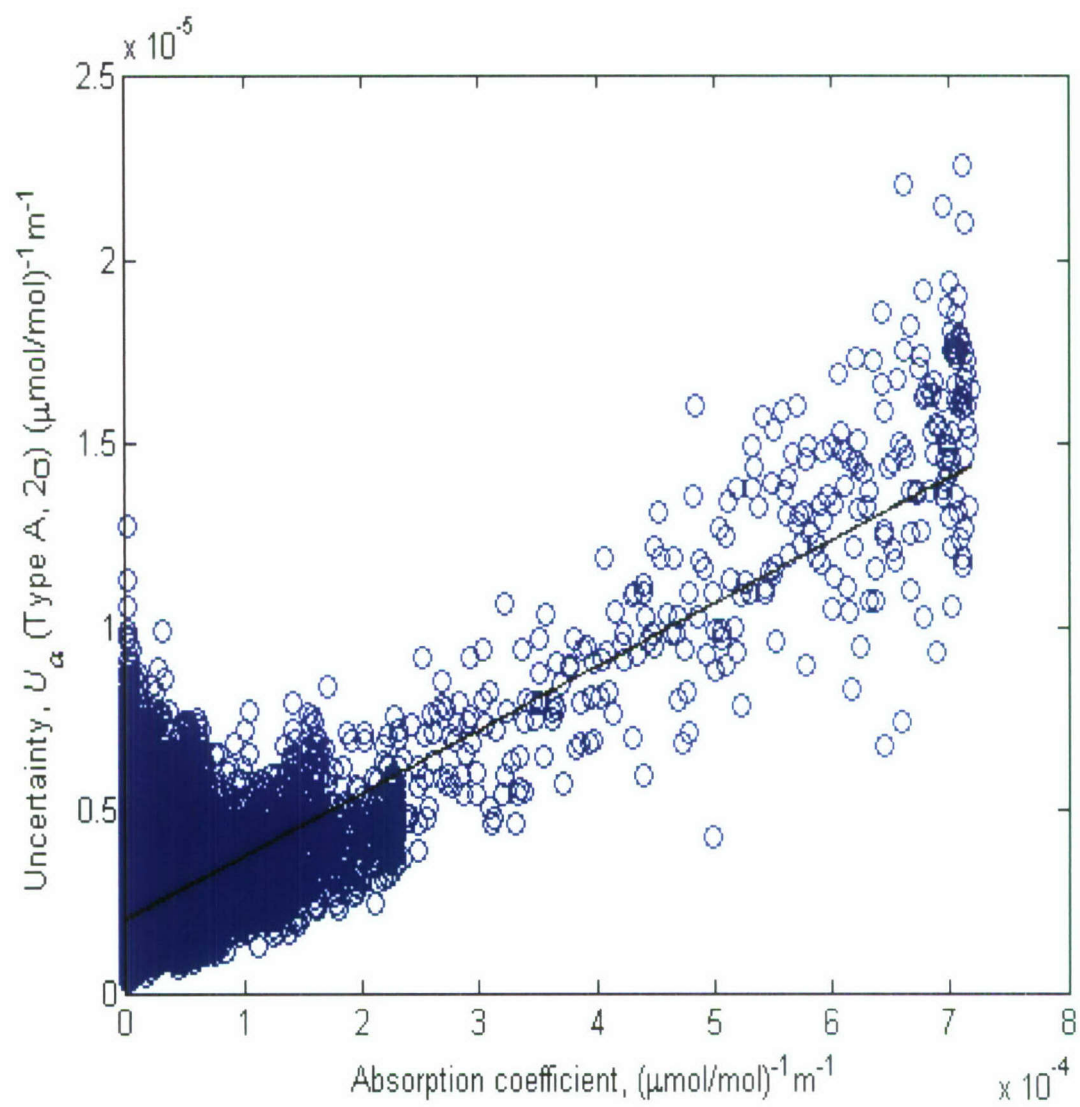


Figure 7. Absorption Coefficient (Abscissa) and Type-A Uncertainty, 2σ , for HD

Table 2. Type-A Statistical Uncertainty for HD Vapor-Phase Absorptivity Coefficient

Type A $2\sigma \approx ma + b$	
Slope m	Intercept b
1.72×10^{-2}	2.03×10^{-6}

Type-B estimated standard errors, their sources, and the combined Type A and B uncertainties are provided in Table 3. The expanded combined Type B uncertainty was computed using eq 2

$$\Delta_B = (\Delta L^2 + \Delta T^2 + \Delta P^2 + \Delta FTIR^2 + \Delta NL^2 + \Delta MR^2)^{1/2} \quad (2)$$

The expanded uncertainty, Type-A + B, was computed with eq 3

$$U_{A+B} = (\Delta_B^2 + \Delta_A^2)^{1/2} * 2 \quad (3)$$

The sources of uncertainty and their fractional values as well as an explanation of the symbols in eq 1 are given in Table 4. Among the Type B uncertainties, the purity of the vapor dominates at 0.015 (1σ).

Table 3. Uncertainties in Absorptivity Coefficient of HD from ECBC Data where $\alpha \geq 0.0000716 \text{ (}\mu\text{mol/mol)}^{-1} \text{ m}^{-1}$

Symbol	Fractional deviation	Source
ΔL	0.005	Pathlength
ΔT	0.0006	Temperature of White cell
ΔP	0.0003	Pressure
$\Delta FTIR$	0.0005	Drift in spectrometer
ΔNL	0.01	Nonlinearity in detector
ΔMR	0.005	Mass rate
ΔD	0.0075	Dilution rate
Δpurity	0.015	Purity of feedstock
Δ_B	0.021	Combined type B (1σ)
Δ_A	0.020	Type-A deviation (1σ)
U_{A+B}	0.057	Combined Type A+B, expanded to 2σ

Comparison of data between laboratories, especially when obtained using different methods, can be useful in assessing the experimental methods and for validating the accuracy of the data. One other source for the high resolution absorptivity coefficient of *bis*-(2-chloroethyl) sulfide for comparison to the data acquired at ECBC is that obtained by Pacific Northwest National Laboratory (PNNL) at Dugway Proving Ground.⁷ The PNNL database includes a detailed discussion of experimental methods and statistical processing. Each absorptivity coefficient spectrum is provided with a metadata file listing physical data for the compound, temperature and pressure range, number of individual spectra included in the fit of the absorptivity coefficient, and Type A and Type B uncertainties.

As can be seen in Figure 8, the spectra from ECBC and PNNL are qualitatively similar. Both the PNNL and our laboratories have undertaken an extensive effort to ensure the wavelength accuracy of the Bruker IFS-66V spectrometers used to acquire spectra, and that deviations average <1 part-per-million in the mid-infrared. Indeed, we have in the past used spectra of compounds exhibiting significant rotational fine structure that had been acquired by PNNL to perform spectral subtraction of spectra obtained in our laboratory with few residual features remaining. When the spectra are expanded within the range of 4000-550 cm^{-1} , it is possible to see differences in the baselines of the two spectra (Figure 9). These are more prominent in the vicinity of 2400 cm^{-1} and near the low frequency cutoff at 600-550 cm^{-1} . In the fingerprint region (Figure 10), there are peaks in the PNNL spectrum from a possible impurity in the vicinity of 1000 cm^{-1} , as well as a shift in the frequency of the CH₂ scissoring band from 1454 to 1445 cm^{-1} .

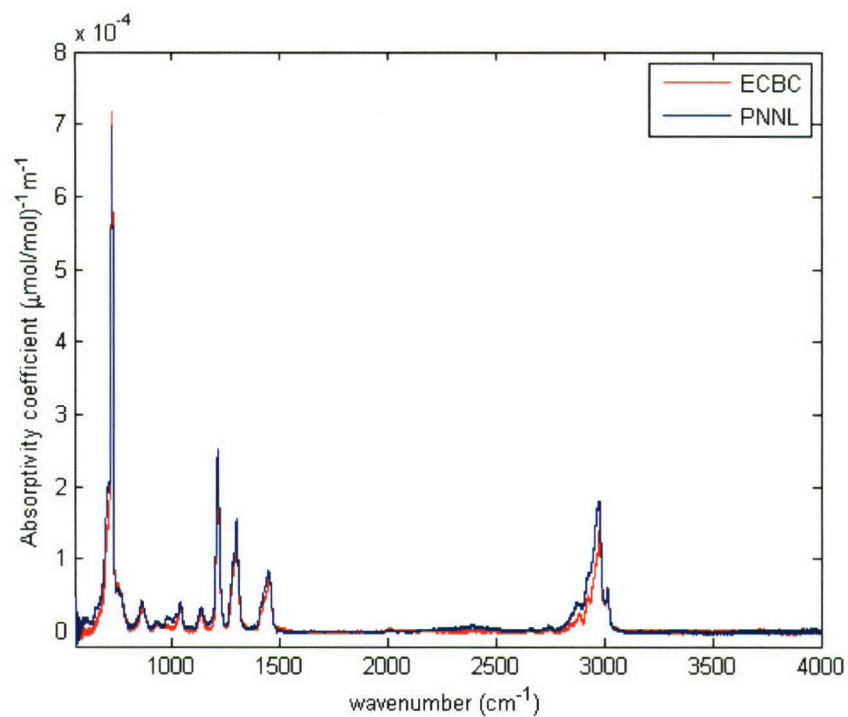


Figure 8. Absorptivity Coefficient of Vapor-Phase HD from ECBC (red) and PNNL (blue)

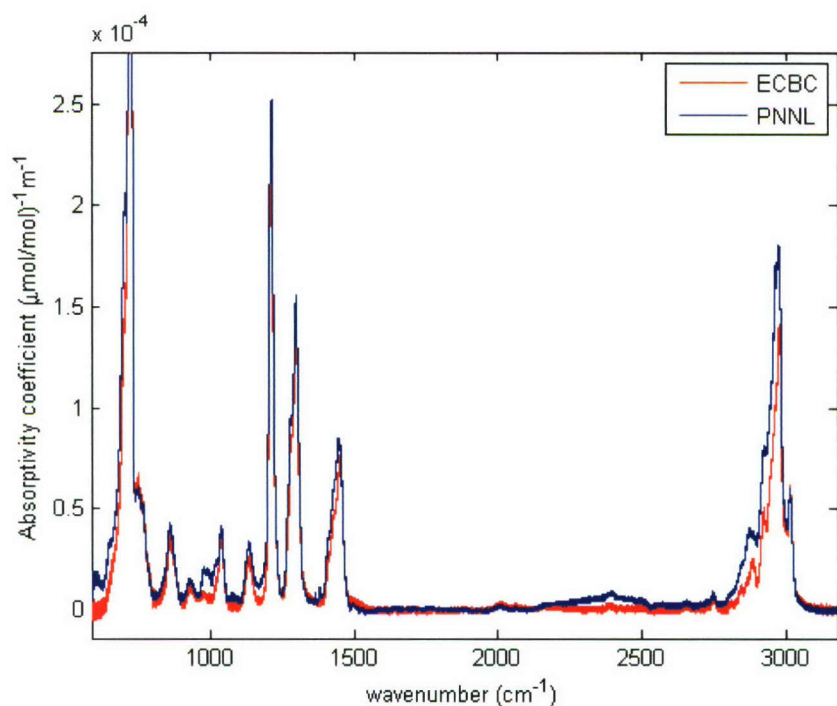


Figure 9. Absorptivity Coefficient Spectra of HD Vapor from ECBC (red) and PNNL (blue). Spectra are zoomed to show the differences in the baselines, particularly near the low frequency cutoff and $\sim 2400 \text{ cm}^{-1}$.

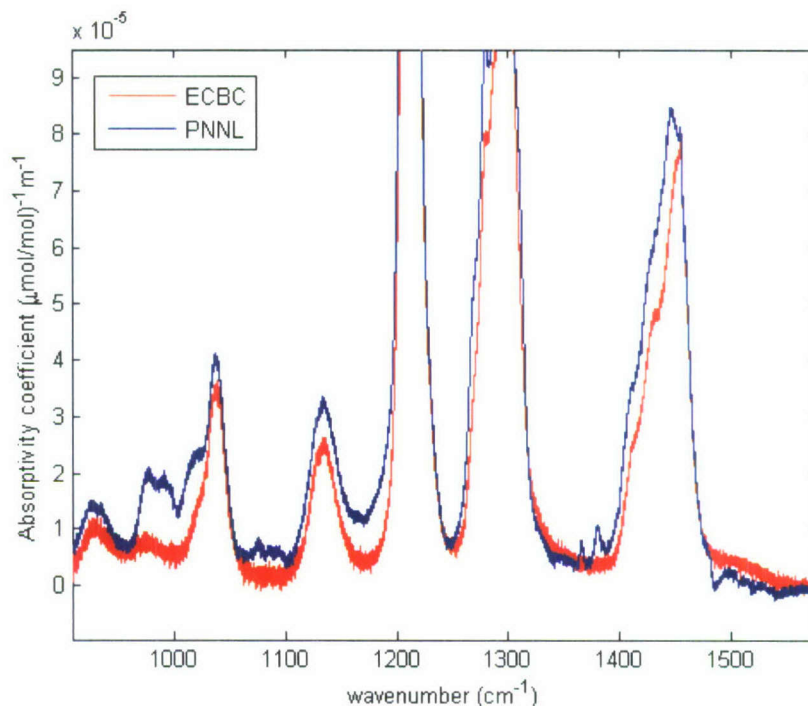


Figure 10. Absorptivity Coefficient Spectra from ECBC (in red) and PNNL (in blue). Spectra are zoomed into the fingerprint region. Note an apparent impurity at $\sim 1020\text{-}920\text{ cm}^{-1}$ and a shift in the frequency of the CH₂ scissoring vibration from 1454 to 1445 cm^{-1} .

One prominent impurity, 1,4-dithiane (DTH), present in both the PNNL composite spectrum and the raw spectra from our laboratory, can be readily identified by a strong, narrow band at 2955.4 cm^{-1} . We recently acquired the absorptivity coefficient spectrum of 1,4-dithiane in the vapor-phase. Before computing the absorptivity coefficient, the features of the DTH were removed from individual spectra of HD using spectral subtraction and adjusted CL products were computed for the individual spectra that accounted for the concentration of the impurity in the spectra. Correcting the PNNL composite spectrum for 1,4-dithiane reduced the integrated area of the spectrum by 1%.

Differences in the baselines of the spectra from ECBC and PNNL may arise from the 7th order polynomial baseline correction method used by PNNL. Because we have rarely observed baseline changes of $A > 0.001\text{-}0.002$ [$A = -\log(I/I_0)$], we have taken a rather conservative approach. We use a MatLab baseline correction algorithm employing linear least squares to fit the baseline, generally to no more than 2 or 3 points. Data taken in our laboratory show this to be satisfactory even in cases of baseline shifts significantly greater than we typically observe. After performing a multipoint linear correction on the PNNL spectrum, the baselines of the two spectra were sufficiently similar to improve the qualitative and quantitative comparison of the two spectra, although differences were still seen.

The PNNL infrared database includes the imaginary refractive index $[i(K)]$ of liquid HD computed from the quantitative transmission spectrum. The absorptivity coefficient of HD can be obtained using eq 4

$$\alpha = \frac{cm^2}{\ln(10)(mol)} (4\pi(\bar{\nu})K(\bar{\nu})) \quad (4)$$

The absorptivity coefficient spectrum thus obtained was then recomputed to units of $(g/cm^3)(\mu m)$ using the molecular weight of HD, 159.2.

When the PNNL and ECBC vapor-phase spectra are overlaid (Figures 11 and 12), it is possible to observe what appears to be a correspondence between features in the PNNL condensed and vapor-phase spectra. Differences in frequencies of absorption bands are common between vapor-phase and condensed-phase spectra. Typically, more electronegative or polar bands, or those subject to hydrogen bonding are shifted to the blue (i.e., higher frequency, lower wavelength) in the vapor-phase, with smaller shifts in less polar bands.^{8,9} This is apparent in the spectra of HD, in which the C-Cl stretch is observed at 721 cm^{-1} in the vapor-phase and at 702 cm^{-1} in the condensed-phase. The effect on the less polar methylene scissoring vibration is less pronounced, with a shift of only 12 wavenumbers. The PNNL vapor-phase spectra were acquired using a syringe pump to introduce the liquid compounds into a heated finger swept by carrier gas at 10-15 L/min, potentially partially aerosolizing the materials.

We then used spectral subtraction to remove the features apparently arising from the presence of condensed-phase material in the vapor-phase spectrum from PNNL. The result of the subtraction can be seen in Figures 13 and 14. Although the result is not ideal because of the lower resolution of the liquid-phase spectrum vis-à-vis the vapor-phase spectrum, the liquid-subtracted PNNL spectrum is qualitatively more similar to the ECBC spectrum. Unassigned peaks, however, are still present in the PNNL spectrum around 1000 cm^{-1} and $1390\text{-}1350\text{ cm}^{-1}$. The latter vibrations are generally assignable to methyl (CH_3) deformations, not present in HD, which has only CH_2 . A common impurity in HD is 2-chloroethyl ethyl sulfide (CEES), which has a terminal methyl. In addition to a band at $\sim 1390\text{ cm}^{-1}$, not seen in the vapor-phase spectrum of HD, CEES has a band at $\sim 975\text{ cm}^{-1}$ that is nearly 40 times more intense than seen in HD, which may account for some, but not all, of the residual differences in the PNNL and ECBC spectra.

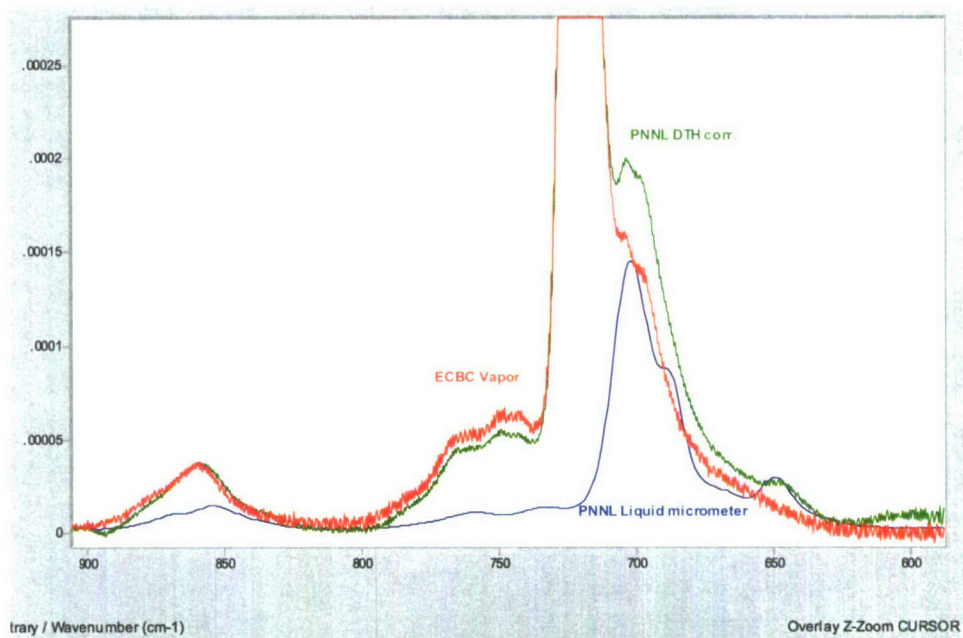


Figure 11. Vapor-Phase Absorptivity Coefficients of HD from PNNL (green) and ECBC (red), and the Liquid Absorptivity Coefficients (blue). The C-Cl stretch is seen at a Δ of 19 wavenumbers in the vapor-phase vis-à-vis the condensed-phase.

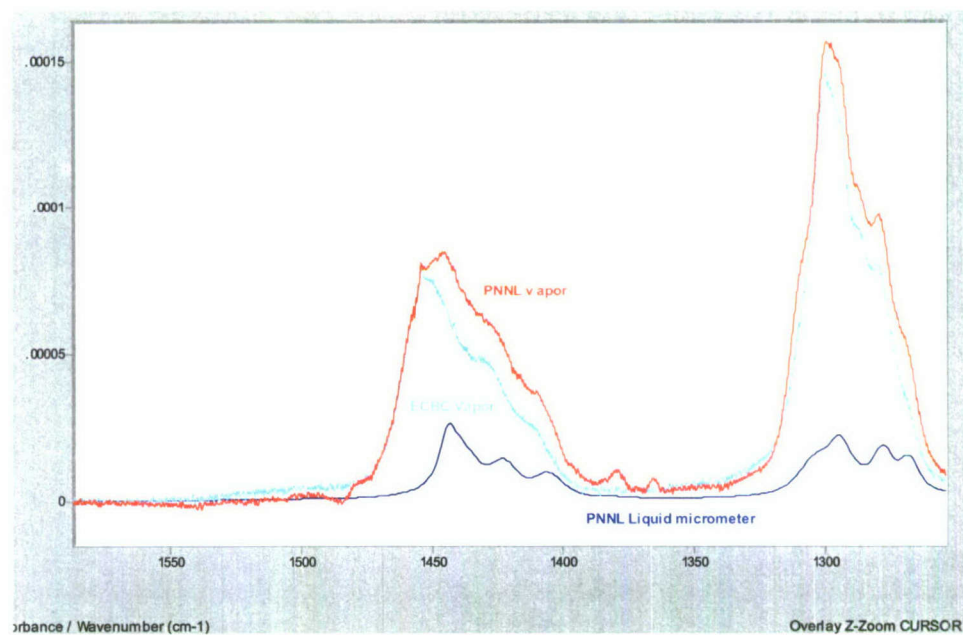


Figure 12. Vapor-Phase Absorptivity Coefficients of HD from PNNL (red) and ECBC (light blue), and the Liquid Absorptivity Coefficients (dark blue). The methylene scissoring vibration is seen at a Δ of 12 wavenumbers in the vapor-phase vis-à-vis the condensed-phase.

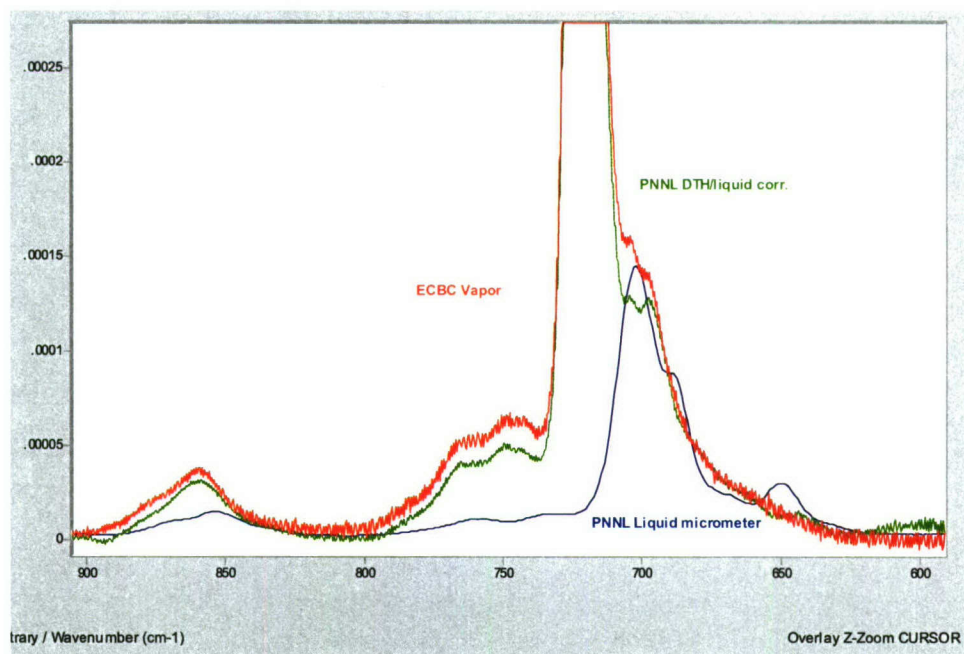


Figure 13. Vapor-Phase Absorptivity Coefficients of HD from PNNL after Spectral Subtraction (green) and ECBC (red), and the Liquid Absorptivity Coefficient (blue).

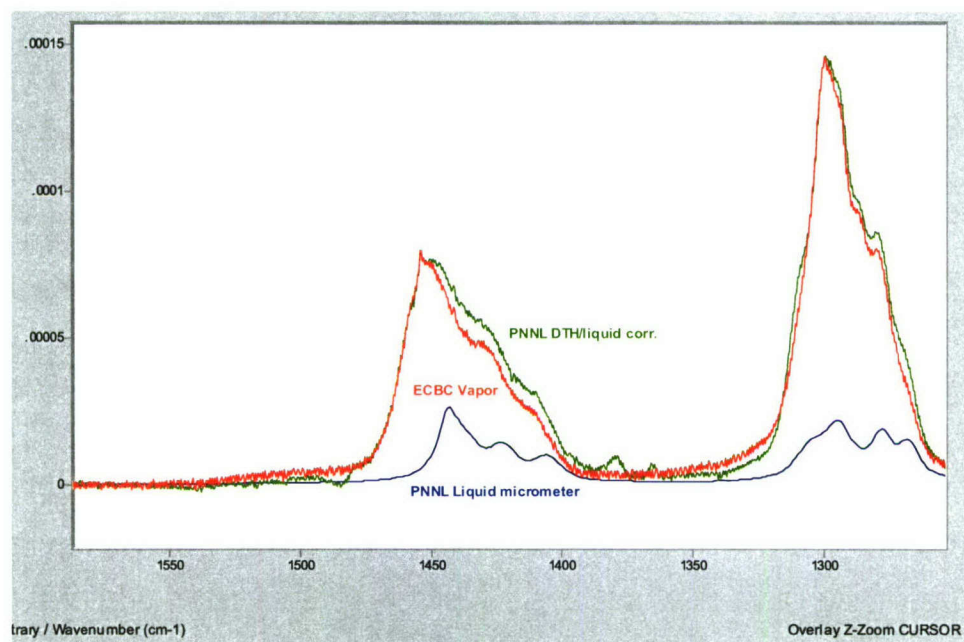


Figure 14. Vapor-Phase Absorptivity Coefficients of HD from PNNL after Spectral Subtraction (green) and ECBC (red), and the Liquid Absorptivity Coefficient (blue). The peak corresponding to CH_2 scissoring is now seen at the same frequency in both vapor-phase spectra.

The ratio of the CH stretch ($3000\text{--}2800\text{ cm}^{-1}$) is proportionately more intense in the PNNL spectrum than in the ECBC spectrum. Table 4 shows a comparison between the ratios of CH and C-Cl bands for the two spectra. The instrument used in the PNNL work was modified by the addition of a second aperture in order to correct for artifacts arising from double modulation and heating of the aperture by the source, which can lead to a distorted absorption line shape that shows a “tailing” to lower frequencies.¹⁰ The authors of the referenced study noted that the artifacts generally tended to increase the integrated areas of peaks in the fingerprint region relative to those at higher wavenumbers. The National Institute of Standards and Technology has used an unmodified Bruker IFS-66V infrared spectrometer to compile a quantitative database.¹¹ An intercomparison of data for 12 compounds between NIST and PNNL showed that, with one exception, deviation in the integrated band strengths was $<2.5\%$. The authors have attributed the small apparent magnitude of the artifacts to the use of a slightly large aperture used for acquiring the NIST data (2.0 vs. 1.5 mm) and the lower throughput induced by the use of a multipass gas (White) cell in the NIST study. The deviation seen in Table 4 is, in any case, much larger than that noted for the unmodified PNNL instrument. Furthermore, the data in Reference 10 were obtained using a 20-cm cell, and those in Table 4 were acquired using a multipass cell. Artifacts arising from double modulation and aperture heating thus apparently cannot account for the deviations noted.

Table 4. Ratios of CH to C-Cl in Vapor-Phase Spectrum from ECBC and Spectrally Subtracted Spectrum from PNNL

	PNNL	ECBC
CH	0.01397	0.00911
C-Cl	0.01924	0.01728
CH/C-Cl	0.726	0.527

The band at 1037 cm^{-1} , although weak, is of interest because of its proposed use as an identification and quantitation band for LIDAR measurements. This band is present as well in the condensed-phase spectrum of HD and is accompanied by a second band at 1021 cm^{-1} , about half the intensity of the higher frequency vibration, which can also be seen in the PNNL vapor-phase spectrum (Figure 15). Spectral subtraction of liquid HD reduced the intensity of this band in the PNNL spectrum by $(0.000040\text{--}0.00003)/0.000033 \times 100 = 21\%$ (vis-à-vis 0.000034 in the ECBC spectrum).

By computing the integrated areas of the PNNL vapor-phase spectrum before and after subtracting the liquid-phase spectrum, it is possible to estimate the proportion of liquid in the vapor-phase spectrum. The integrated area of the uncorrected spectrum is 0.05120; the area of the corrected spectrum is 0.0460: $0.05120\text{--}0.0460 = 0.0591$, corresponding to an average pathlength for undiluted HD of $0.045\text{ }\mu\text{m}$.

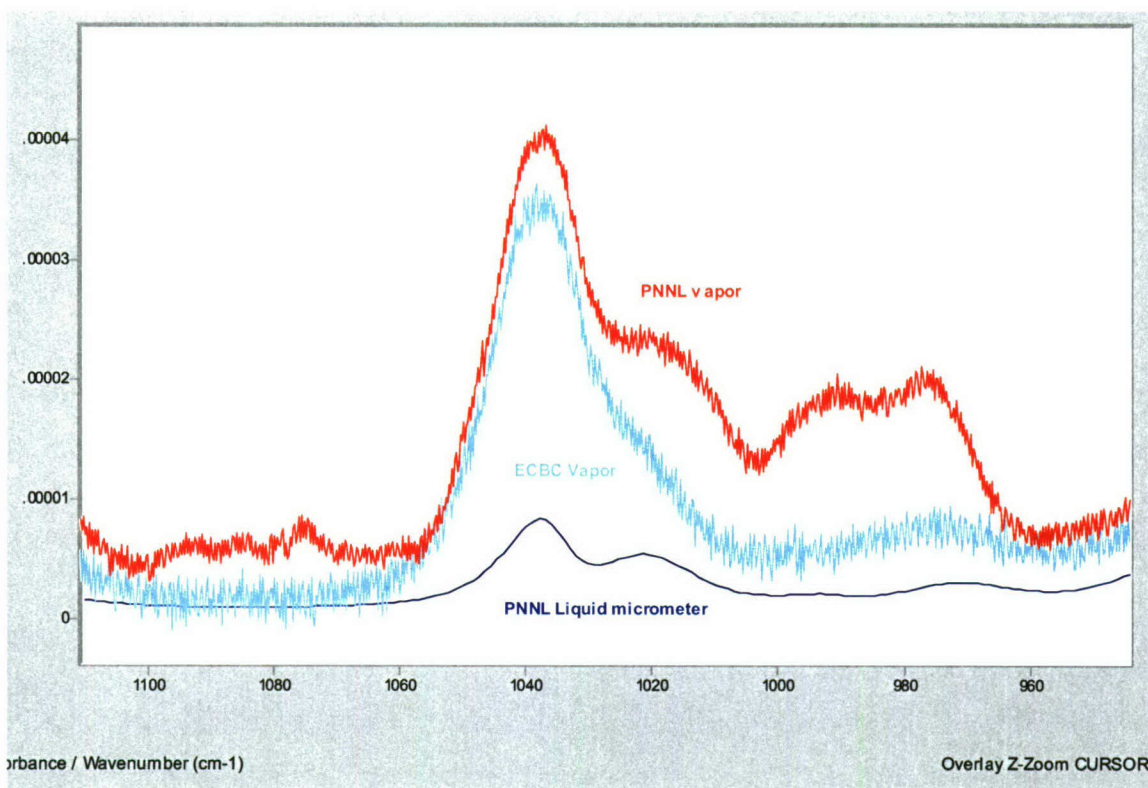


Figure 15. Band at 1037 cm^{-1} in Vapor-Phase Spectra of HD from PNNL (red) and ECBC (light blue) and Liquid-Phase Spectrum from PNNL. After spectral subtraction, the intensity of this band is reduced by 18%.

A comparison of the integrated areas in the ECBC and PNNL spectra before and after spectral subtraction of 1,4-dithiane and liquid HD is shown in Table 5. The data are for the range $4000\text{--}550\text{ cm}^{-1}$. The metadata file associated with the PNNL vapor-phase absorptivity coefficient of HD indicates uncertainties of 3.5% (Type-A) and $\leq 10\%$ (Type-B). The difference calculated for the integrated areas of the PNNL (subtracted) and ECBC data seen in the last column of Table 5 is well within the limits of the combined uncertainties of the experimental methods

Table 5. Comparison of Integrated Vapor-Phase Absorptivity Coefficient Spectrum of HD from PNNL and ECBC

PNNL	ECBC	(PNNL- ECBC)/ECBC X 100	PNNL (after spectral subtraction)	ECBC	(PNNL- ECBC)/ECBC X 100
0.05746	0.04390	30.9%	0.0460	0.04390	4.8%

5. CONCLUSIONS

The vapor-phase absorptivity coefficient of *bis*-(2-chloroethyl) sulfide (HD) was measured within the range 4000-550 cm^{-1} . Combined uncertainties, expanded to 2σ , are 5.7% of the absorptivity coefficient at intensities $\geq 5\%$ of the most intense absorption feature.

Blank

LITERATURE CITED

1. Barrett, W.J.; Dismukes, E.B. *Infrared Spectral Studies of Agents and Field Contaminants*; 9299-2018-11; Southern Research Institute: Birmingham, AL, 1969; UNCLASSIFIED Report (AD-395 378).
2. Buchanan, J.H.; Buettner, L.C.; Tevault, D.E. *Ambient Volatility of Bis-(2-chloroethyl) Sulfide*; ECBC-TR-580; U.S. Army Edgewood Chemical Biological Center: Aberdeen Proving Ground, MD, 2007; UNCLASSIFIED Report (AD-B328 723).
3. Tevault, D.E.; Keller, J.; Parsons, J. *Vapor Pressure of Dimethyl methylphosphonate*; ECBC-SP-004; U.S. Army Edgewood Chemical Biological Center: Aberdeen Proving Ground, MD, 1999; UNCLASSIFIED Report (AD-E491 779).
4. Williams, B.R.; Ben-David, A.; Green, N.; Hulet, M.S.; Miles, R.N.; Samuels, A.C. *Validation and Support of a Quantitative Vapor-Phase Infrared Instrument Facility and Generation of a Library of Chemical Warfare and Related Materials by Fourier Transform Infrared Spectroscopy*; ECBC-CR-076; U.S. Army Edgewood Chemical Biological Center: Aberdeen Proving Ground, MD, 2006; UNCLASSIFIED Report (AD-A471 712).
5. Williams, B.R.; Samuels, A.C.; Miles, R.W.; Hulet, M.S.; Ben-David, A. ECBC Quantitative Vapor-Phase Infrared Spectral Database, In *Proceedings of the 2007 Scientific Conference on Chemical & Biological Defense Research, 13-15 November 2007*; SOAR-07-20; Chemical, Biological, Radiological & Nuclear Defense Information Analysis Center: Gunpowder, MD, 2008.
6. Grubbs, F. Procedures for Detecting Outlying Observations in Samples. *Technometrics*, **1969**, *11*(1), pp 1-21.
7. DOE/PNNL Infrared Spectral Library, Release 11.0; Department of Energy/Pacific Northwest National Laboratory: Richland, WA, 2006.
8. Griffiths, P.R.; de Haseth, J.A. *Fourier Transform Infrared Spectrometry*; Wiley-Interscience: New York, 2007.
9. Nyquist, R.A. *The Interpretation of Vapor-Phase Infrared Spectra*; Sadtler Research Laboratories: Philadelphia, 1984.
10. Johnson, T.J.; Sams, R.L.; Blake, T.A.; Sharpe, S.W.; Chu, P.M. Removing Aperture-Induced Artifacts from Fourier Transform Infrared Intensity Values. *Appl. Opt.*, **2002**, *41*, p 2831.
11. Chu, P.M.; Guenther, F.R.; Rhoderick, G.C.; Lafferty, W.J. The NIST Quantitative Infrared Database. *J. Res. Natl. Inst. Stand. Technol.*, **1999**, *104*, p 59.